CONF-810531--25

DAMAGE STRUCTURE IN NIMONIC PE16 ALLOY ION BOMBARDED TO HIGH DOSES AND GAS LEVELS*

K. Farrell and N. H. Packan

Oak Ridge National Laboratory
Oak Ridge, Tennessee 37830

The Nimonic PE16 alloy in solution-treated-and-aged condition was bombarded simultaneously with nickel ions and α and deuteron beams at 625°C to doses of 80 to 313 dpa at He/dpa = 10 and D/dpa = 25. Microstructural changes consisted of the introduction of dislocations and of cavities, and the redistribution of γ′ precipitates to these defects. Cavitational swelling remained below 1%. Cavities were represented by several distinct size classes, the smaller ones believed to be gas bubbles, and some larger ones associated with preferred growth of precipitate. Formation of bubbles at grain boundaries, and large cavities at incoherent twins intensified the possibility of mechanical separation of interfaces under high-gas irradiation conditions.

INTRODUCTION

Swelling and phase instability in alloys irradiated in the range 0.25 to 0.5 T_m are sensitive to the presence of gases, particularly helium [1]. Large quantities of helium and hydrogen will be generated by (n,α) and (n,p) reactions in the first wall of a MFR, and some will be injected from the plasma. The Nimonic PE16 alloy is a candidate wall material that displays good swelling resistance during neutron [2–7] and heavy ion [4,6,8–10] bombardments, but suffers phase redistribution. The test conditions have embraced moderate displacement doses and low-to-high helium levels, but not the simultaneous high dose-high gas conditions expected in a first wall. The estimated [11] gas generation rates in a first wall of Nimonic PE16 alloy are 20 appm He/dpa and 66 appm H/dpa; an exposure of 40 MW yr m^{-2} would cause a displacement level of 470 dpa. We have studied ion damage in PE16 alloy under conditions approaching these.

EXPERIMENTS

The composition of the alloy was 43.8 wt % Ni, 34 Fe, 16.6 Cr, 3.4 Mo, 1.1 Al, 1.0 Ti, and 0.06 C. TEM blanks, 3 mm diam × 0.5 mm thick, were punched from cold-rolled stock, and were given a standard heat treatment consisting of solution anneals at 1080 and 890°C followed by aging for 7 h at 750°C to develop a fine precipitate of γ′ phase. Following diamond lapping to a 0.1 μm finish and a light electropolish, the specimens were bombarded at 625°C with nickel, helium, and deuterium ions simultaneously, as described elsewhere [12]. The displacement rate was in the range 2×10^{-4} to 7×10^{-3} dpa s^{-1}. The specific displacement levels and gas implantation rates are given at the appropriate places in the Results section. Because the experiments contained other alloys, the gas/dpa ratios are compromise values to suit all the alloys, and are somewhat lower than the estimated MFR first wall value for PE16 alloy. Nevertheless, they are of the required order of magnitude. TEM observations were made at the peak damage depth of ~0.7μm.

RESULTS

Unbombarded Controls

The as-heat-treated alloy consisted of equiaxied grains with some annealing twins and with a finely-dispersed precipitate of γ′ phase. The γ′ precipitate particles were coherent, near-spherical, ~15 nm diameter, and difficult to observe under bright field examination. They were seen best in dark field mode [Fig. 1(d)]; their concentration was about 10^{22} m^{-3}. Grain boundaries contained much coarser particles, 70–250 nm in size, spaced non-uniformly on the boundaries. Specimens held at 625°C for 12 h to simulate the heating experienced during ion bombardment showed no discernible changes in microstructure.

80 dpa, He/dpa = 11, D/dpa = 28

Two specimens were available in this condition. Unfortunately, both exhibited fine etching and surface films during preparation of TEM foils. Diffraction rings from these artifacts tended to coincide with the γ′ spots, interfering with dark field imaging. There seemed, however, to be no gross changes in the γ′ precipitates. The most obvious changes were the introduction of dislocations and cavities (Table 1). The dislocations were in the form of a tight network. The cavities were uniformly distributed and were in two distinct size classes — a low concentration of mean diameter ~20 nm and a much higher concentration (~3×10^{22} m^{-3}) of very small ones at about 3 nm. There was no association of the cavities with the original γ′ precipitates.

*Research sponsored by the Division of Materials Sciences, U. S. Department of Energy under contract W-7405-eng-26 with the Union Carbide Corporation.

YS 12188

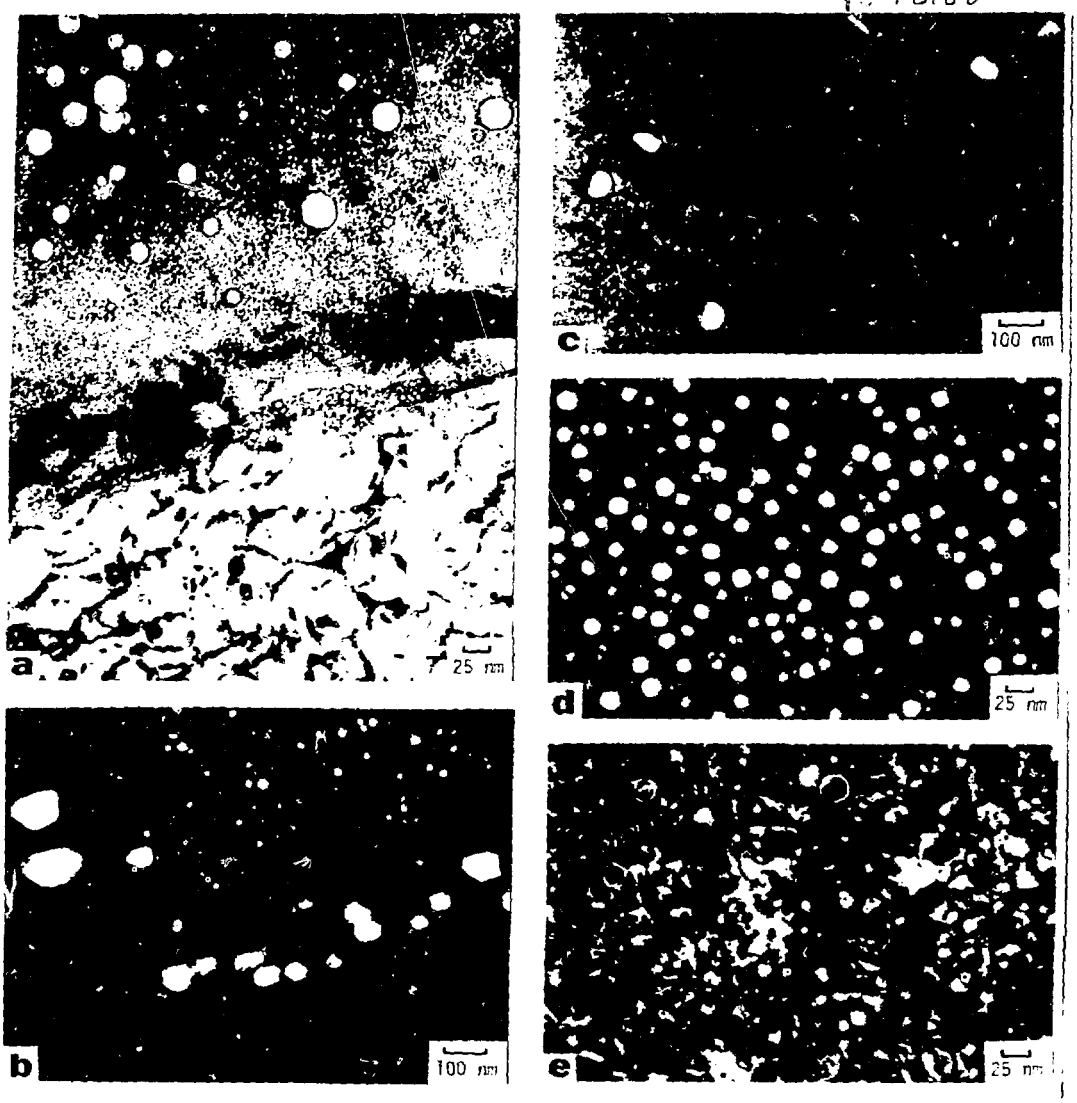

Fig. 1 (a) Dislocations, grain boundary cavities, and matrix cavities and (b) large cavities on incoherent twins, after 180 dpa. (c) Large matrix cavities and attached precipitates produced at 313 dpa. (d) and (e) matrix γ' precipitates shown under dark field conditions in the unirradiated control and the 180 dpa specimens, respectively.

There were no 20 nm cavities within ~120 nm of grain boundaries. The smaller, 3 nm cavities persisted right up to the grain boundaries, as did the dislocations. On the grain boundaries there were cavities with mean diameter of 3.5 nm and of quite high planar concentration. Incoherent parts of annealing twins suffered strong preferential etching, suggesting some radiation-induced structural or chemical changes there.

180 dpa, He/dpa = 8.5, D/dpa = 21

There were many more cavities than at the lower dose. The smaller, 3 nm, class were more evident, and many of them were located in strings

TABLE 1. SUMMARY OF CAVITY AND DISLOCATION DATA

Irradiation Conditions	Dislocation Density	Small Matrix Cavities		Medium Matrix Cavities		Large Matrix Cavities		Incoherent Twin Cavities		Grain Boundary Cavities		Swelling
	$\rho(m^{-2})$	$\bar{d}$(nm)	$\bar{N}(m^{-3})$	$\bar{d}$(nm)	$\bar{N}(m^{-3})$	$\bar{d}$(nm)	$\bar{N}(m^{-3})$	$\bar{d}$(nm)	$\bar{N}(m^{-2})$	$\bar{d}$(nm)	$\bar{N}(m^{-2})$	(%)
80 dpa He/dpa = 11 D/dpa = 28	3.5×10^{14}	2.8	3.3×10^{22}	22	4.3×10^{20}	None		Boundaries Etched		3.5	2×10^{13}	0.28
180 dpa He/dpa = 8.5 D/dpa = 21	4×10^{14}	3.2	6.6×10^{22}	20	2.1×10^{20}	None		60–93	4×10^{13}	6	1.2×10^{13}	0.99
313 dpa He/dpa = 10 D/dpa = 25	4.5×10^{14}	6.3	2.2×10^{22}	17	7×10^{20}	62	5×10^{18}	98	2×10^{13}	5.5	2×10^{13}	0.59

on dislocations. The 20 nm class increased in concentration about five-fold without change in mean diameter. Cavities on grain boundaries were roughly doubled in size with no increase in concentration. Examples of matrix and grain boundary cavities are given in Fig. 1(a). The dislocation density was the same as at 80 dpa. Large, facetted cavities, 60–90 nm, were found on incoherent twin faces [Fig. 1(b).]; they were not associated with precipitates. Between 30 and 50% of the incoherent twins harbored these large cavities.

The original, rounded γ' particles within the grains were no longer distinguishable. Instead, there were many and much smaller, irregular-shaped γ' particles, and many of these were located on the radiation-induced dislocations and at cavities [Fig. 1(c)]. Quantitative measurements of these particles were not attempted, but there was no obvious change in volume fraction. The original, large grain boundary particles of γ' remained apparently unchanged, but their surfaces were covered with small cavities.

313 dpa, He/dpa = 10, D/dpa = 25

A third size class of matrix cavities was introduced. A low concentration of relatively large (~60 nm) cavities was formed attached to preferentially-growing particles of γ'. There were no large size matrix γ' particles without cavities, and vice versa. The concentration of small cavities was decreased and their size increased, and the concentration of the 20 nm medium-size cavities was reduced. Large cavities persisted on incoherent twins. Grain boundary cavities seemed to be about the same size as those at 180 dpa but measurement of them was difficult because at this highest dose precipitation at grain boundaries was enhanced to the point where the boundaries were almost completely covered by precipitate. In the grains γ' particles persisted on the dislocations and cavities; some were also observed at sizes and shapes similar to the orginal γ' particles but at very much lower concentration.

DISCUSSION

These observations can be reduced to four main items:

1. Swelling is low. Superior swelling resistance in the Nimonic PE16 alloy is usually manifest as an extended incubation period and restricted concentrations of cavities [9]. Moreover, it has been shown [9,10] that even in the absence of γ', the matrix composition provides good swelling resistance, indicating that the beneficial agents are solutes, not γ' precipitate. Indeed, depletion of solutes by formation of extra γ' during long-term reactor preconditioning is held to be responsible for excessive swelling under subsequent ion bombardment [6]. In the relatively short times involved in the present work there was no obvious increase in the volume fraction of γ' during irradiation, and swelling remained below 1% despite the high displacement doses. The limiting factor was cavity growth, not nucleation, the implanted gases ensuring copious nucleation. In fact, nucleation was *too efficient*. The cavity (vacancy) sink strength, $2\pi Nd$, was significantly greater than the interstitial sink strength denoted by the dislocation density (Table 1). Under such circumstances the cavities are the dominant sink for excess point defects, and recombination there retards cavity growth and swelling [13]. Unfortunately, repression of swelling by promoting excessive cavity nucleation with gases also has the undesirable side effect of introducing grain boundary cavities, as discussed later.

2. Cavities are gas stabilized. The presence of cavities on grain boundaries in the absence of stress is usually considered convincing evidence of gas bubble formation. Such bubbles are plentiful in our specimens. Helium is the most likely culprit since experiments [12] have shown that the implanted deuterium escapes rapidly. Moreover, calculations using the matrix cavity

data from Table 1 and the gas laws with Van der Waals' correction indicate that the specimens contain more than enough helium to stabilize the small cavities as equilibrium bubbles. The amounts of helium required for the 80, 180, and 313 dpa specimens are 216, 510, and 1160 appm, respectively. The corresponding implanted helium levels are 880, 1530, and 3130 appm. To fill *all* of the matrix cavities requires 485, 1825, and 1470 appm He, respectively. So the chances are good that all cavities are helium bubbles, certainly the small ones whose sizes are close to those of the grain boundary bubbles.

3. γ' phase is redistributed. Destruction of the original γ' matrix precipitate and its redistribution to point defect sinks agrees with observations by others [2–8]. As such, it requires little further comment except to point out, following Gelles [14], that these phase changes under short-term ion irradiations may give a misleading impression of those expected under actual MFR irradiation to similar doses; thermal (temporal) coarsening may make a greater contribution under long-term irradiations. Such coarsening may lead to enhanced swelling by changing the sink strength or by cooperative cavity-precipitate growth [15], for which we see some evidence at the highest dose. Long-term irradiation may also lead to solute depletion and increased swelling [6]. Additionally, the considerable build-up of precipitate at grain boundaries at high dose could degrade the mechanical integrity of the boundaries.

4. Interfacial cavities. Perhaps the biggest cause for concern is the interfacial bubbles which could lead to severe helium embrittlement under service stresses and temperature excursions. These bubbles occur in high planar concentrations on grain boundaries, on grain boundary precipitates, and at incoherent parts of annealing twins. Those on the twins are unusual in that they are very much larger than those on grain boundaries. There is no obvious explanation for this exceptional growth. At the grain boundaries the bubble concentrations appear to saturate at about 2×10^{15} m^{-2}, with a mean center-to-center spacing of only 25 nm. They grow with increasing dose (helium concentration) and at the highest dose they occupy ~5% of the grain boundary area. Simple calculations show that their growth is consistent with their absorbing all the helium implanted in a narrow zone only 10 to 15 nm wide on each side of the grain boundary. This, in turn, concurs with the observation that the small matrix cavities extend almost up to the grain boundaries. In fact, their center-to-center spacing is 32 nm, or less, which would agree with a grain boundary denuded zone of <15 nm. Since these matrix cavities are supposedly strong sinks for helium, and they exist on a finely-dispersed scale, this discussion indicates that it will be difficult to keep helium away from grain boundaries by absorbing it at matrix interfacial sinks. The scale of helium trapping (fixing) will need to be very much finer than the already fine level in this irradiated PE16 STA.

ACKNOWLEDGMENTS

We are pleased to recognize the assistance of Dr. M. B. Lewis, Claudette G. McKamey, and John T. Houston with these experiments, and Judy Young for secretarial services.

REFERENCES

[1] Farrell, K., Rad. Effects 53 (1980) 175–194.
[2] Sklad, P. S., Clausing, R. E., and Bloom, E. E., pp. 139–155 in Irradiation Effects on the Microstructure and Properties of Metals, ASTM STP 611, (1976).
[3] Whapham, A. D., Harwell, unpublished work (1976).
[4] Bleiberg, M. L., Bajaj, R., Bell, W. L., and Thomas, L. E., pp. 667–685 in Radiation Effects in Breeder Reactor Structural Materials, Met. Soc. AIME, New York (1977).
[5] Braski, D. N., and Wiffen, F. W., Alloy Development for Irradiation Performance, DOE Report DOE/ET-0058/1, Aug. 1978.
[6] Bajaj, R., Diamond, S., Chickering, R. W., and Bleiberg, M. L., pp. 541–561 in Effects of Radiation on Materials: Tenth Conference, ASTM STP 725, (1981).
[7] Gelles, D. S., pp. 562–582 in Effects of Radiation on Materials: Tenth Conference, ASTM STP 725, ASTM (1981).
[8] Nelson, R. S., Hudson, J. A., and Mazey, D. J., J. Nucl. Mater., 44 (1972) 318–330.
[9] Makin, M. J., Hudson, J. A., Mazey, D. J., Nelson, R. S., Walters, G. P., and Williams, T. M., pp. 645–665 in Radiation Effects in Breeder Reactor Structural Materials, Met. Soc. AIME, New York (1977).
[10] Mazey, D. J., and Nelson, R. S., J. Nucl. Mater., 85 and 86 (1979) 673–675.
[11] Gabriel, T. A., Bishop, B. L., and Wiffen, F. W., Nucl. Technol., 38 (1978) 427–433.
[12] Farrell, K., Lewis, M. B., and Packan, N. H., Scripta Met., 12 (1978) 1121–1124.
[13] Mansur, L. K., Nucl. Technol., 40 (1978) 5–34.
[14] Gelles, D. S., pp. 194–206 in Effects of Radiation on Structural Materials, ASTM STP 683 (1979).
[15] Mansur, L. K., Hayns, M. R., and Lee, E. H., in Proceedings of Symposium on Irradiation Effects on Phase Stability, Pittsburgh, October 5–9, 1980, TMS-AIME (in press).